Proceedings of ICRC 2001: 2018 © Copernicus Gesellschaft 2001

ICRC 2001

# Self consistent particle acceleration in 2D supernova remnant shocks

**A. R. Zakharian[1], G. M. Webb[2], M. Brio[3], and J. R. Jokipii[4]**

[1]ACMS, University of Arizona, Tucson, AZ 85721, U.S.A.
[2]PL, University of Arizona, Tucson, AZ 85721, U.S.A.
[3]Department of Mathematics, University of Arizona, Tucson, AZ 85721, U.S.A.
[4]LPL and Dept. of Planetary Sciences, University of Arizona, Tucson, AZ 85721, U.S.A.

**Abstract.** We present numerical solutions of a two dimensional, self consistent model of cosmic ray modified, supernova remnant shocks developed by Zakharian (2000). The equations of the model consist of the Parker transport equation for the energetic particle momentum distribution function, $f$, including convection, anisotropic diffusion, drifts, and adiabatic energy changes. The transport equation is coupled self consistently, with the equations of ideal magnetohydrodynamics (MHD) describing the thermal plasma, but suitably modified to take into account injection at the shock, and with an extra force $-\nabla p_c$, exerted by the cosmic ray pressure $p_c$ in the momentum equation for the system. The model incorporates anisotropic diffusion of the cosmic rays, including diffusion parallel ($\kappa_\parallel$), and perpendicular ($\kappa_\perp$) to the mean magnetic field, and the role of particle drifts due to the anti-symmetric diffusion coefficient $\kappa_A$. For the case of an initially uniform background magnetic field, the anisotropic diffusion of the cosmic rays leads to an anisotropic spatial distribution of thermal plasma, cosmic rays and magnetic field. The shock is quasi-parallel over the poles ($\theta = 0^\circ$), and quasi-perpendicular near the equator ($\theta = 90^\circ$), where $\theta = 0^\circ$ corresponds to the initial magnetic field direction. The evolution of the SNR shock, and the momentum distribution $f(\mathbf{r}, p, t)$ of the energetic particles are investigated. The dependence of the solutions and acceleration rate at the shock on the parameter $\eta = \kappa_\perp/\kappa_\parallel$ and the shock obliquity $\theta$ are studied in detail.

## 1 Introduction

The earlier numerical work on diffusive shock acceleration used simplified one dimensional fluid model description of the cosmic rays (Jones and Kang (1990), Dorfi (1990)) or transport equation models in either plane shock (Falle and Giddings (1987)) or test-particle approximation (Jokipii and Ko (1987)). These and other numerous studies, suggested that diffusive shock acceleration could convert around 10-15% of the SNR kinetic energy into cosmic ray energy.

More physically realistic models have been used in the numerical investigation of diffusive particle acceleration in spherical SNR shocks (Kang and Jones, 1991; Berezhko et al., 1996). Direct numerical solution of the transport equation with constant and weakly momentum dependent ($\kappa \sim p^{1/4}$) diffusion coefficient models in Kang and Jones (1991) suggested that cosmic rays can absorb as much as 30% of the explosion kinetic energy, and indicated that a power law with slope $\sim 4.3$ may be established up to the energies of $10^{14}$ eV. Berezhko et al. (1996) investigated the problem with the momentum dependent diffusion coefficient $\kappa \sim p$ which corresponds to the Bohm limit for high energy particles. This regime is characterized by small diffusion coefficients at low energies, when the mean free path of the particle is comparable to the gyroradius, and can be expected if the region near the shock front is highly turbulent. Depending on the injection rate, 20-50% of total blast energy can be transfered to cosmic rays.

Previous studies considered one dimensional, planar or spherical hydrodynamic shocks, with an inherent assumption that the turbulence scattering the particles was sufficiently strong that an isotropic diffusion model could be used. We use a new self-consistent, coupled MHD and particle transport code to follow the evolution of cosmic ray modified shocks in two spatial dimensions. Multi-level solution adaptive mesh refinement provides enhanced resolution around the shock wave. This allows us to consider particle transport both parallel and perpendicular to the field lines.

## 2 The model

To investigate diffusive acceleration of particles in two dimensional supernova shocks, we model the plasma dynamics using the ideal MHD equations coupled to the diffusive cosmic ray transport equation. The cosmic rays are assumed to be a hot, low density gas with a significant pressure, but

*Correspondence to:* G.M. Webb (gwebb@lpl.arizona.edu)

with a negligible mass flux. The isotropic distribution function $f(\mathbf{r}, p, t)$ for the cosmic rays at position $\mathbf{r}$, momentum $p$ at time $t$ satisfies the diffusive cosmic ray transport equation (Krymskii, 1964; Parker, 1965; Skilling, 1975):

$$\frac{\partial f}{\partial t} + (\mathbf{u} + \mathbf{V}_d) \cdot \nabla f - \nabla(\kappa \nabla f) - \frac{1}{3} \nabla \cdot \mathbf{u} \frac{\partial f}{\partial \ln p} = Q, \quad (1)$$

where $\mathbf{u}$ is background plasma velocity; $\kappa$ is the symmetric energetic particle diffusion tensor including the effects of anisotropic diffusion parallel and perpendicular to the background magnetic field $\mathbf{B}$,

$$\mathbf{V}_d = \nabla \times \left( \kappa_A \frac{\mathbf{B}}{B} \right), \quad (2)$$

is the effective drift velocity of the particles, and $\kappa_A$ is the antisymmetric component of the diffusion tensor (in the weak scattering limit $\kappa_A = v r_g / 3$, where $v$ and $r_g$ are particle speed and gyroradius). The term $Q$ on the right hand side of (1) represents injection of particles from thermal pool. It is sufficient to consider a distribution function that describes only protons, the dominant species of the ionized component in the interstellar medium.

The cosmic rays in the model are coupled self-consistently with the equations for the background plasma flow:

$$\frac{\partial \rho}{\partial t} + \nabla \cdot (\rho \mathbf{u}) = 0, \quad (3)$$

$$\frac{\partial \mathbf{u}}{\partial t} + \mathbf{u} \cdot \nabla \mathbf{u} = -\frac{\nabla(p_g + p_c)}{\rho} + \frac{(\nabla \times \mathbf{B}) \times \mathbf{B}}{\mu \rho}, \quad (4)$$

$$\frac{\partial p_g}{\partial t} + \mathbf{u} \cdot \nabla p_g + \gamma_g p_g \nabla \cdot \mathbf{u} = (\gamma_g - 1) S, \quad (5)$$

$$\frac{\partial \mathbf{B}}{\partial t} = \nabla \times (\mathbf{u} \times \mathbf{B}), \quad (6)$$

$$\nabla \cdot \mathbf{B} = 0. \quad (7)$$

The above equations consist of: the mass continuity equation for the thermal gas (3); the total momentum equation for the system (4), in which the cosmic rays modify the background flow by their pressure gradient $-\nabla p_c$; the co-moving gas energy equation (5) is written in terms of the gas pressure $p_g$ and gas adiabatic index $\gamma_g$, and the loss term $S$ on the right hand side of (5) represents the loss of energy of the thermal gas to the cosmic rays due to injection; Maxwell's equations in the MHD limit, namely Faraday's law (6) and Gauss's equation (7) governing the magnetic field induction $\mathbf{B}$. In (4), the cosmic ray pressure $p_c$ is related to the energetic particle distribution function by the equation

$$p_c = \frac{4\pi c}{3} \int_{p_l}^{\infty} dp \frac{p^4 f}{\sqrt{p^2 + m^2 c^2}}, \quad (8)$$

where $p_l$ is a lower boundary in momentum space defining the cosmic ray gas. Particles with momentum $p > p_l$ are regarded as cosmic-ray particles satisfying the diffusive transport equation (1), whereas particles with momenta $p < p_l$ comprise the thermal plasma. The injection term $Q$ and energy change term $S$ are related by:

$$Q = -\frac{1}{3} p_{inj} f(\mathbf{r}, p_{inj}, t) \nabla \cdot \mathbf{u} \delta(p - p_{inj}), \quad (9)$$

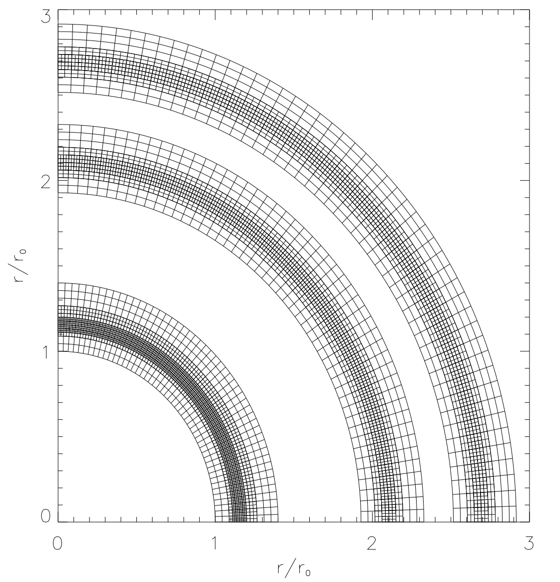


**Fig. 1.** AMR grid structure evolution, $t/t_0$ = 1.0, 4.5, 8.0.

$$S = \frac{4\pi}{3} (p^3 T f)_{p=p_{inj}} \nabla \cdot \mathbf{u},$$

where $p_{inj}$ and $T_{inj}$ are the injection momentum and kinetic energy of the particles. We follow Falle and Giddings (1987) and set $\nabla \cdot \mathbf{u} = (u_1 - u_2)\delta(r - r_{sh})$ at the subshock. In the present work we use the injection speed $v_{inj} = \xi v_{sh} (\kappa_\parallel / \kappa_{nn})^{1/2}$, where $\kappa_{nn}$ is the effective diffusion coefficient normal to the shock surface, $v_{sh}$ is the shock speed and $\xi$ is a parameter of order unity. This estimate can be considered as a lower limit on the injection rate, that neglects pre-acceleration processes, which can enhance the particle distribution at low energies above the value expected from a Maxwellian distribution. More realistic injection models (Malkov and Völk, 1995; Gieseler et al., 1999) can be incorporated into the model, but will not be considered here.

## 3 Numerical Method

Equations (1) and (3)-(7) are discretized in spherical polar $(r, \theta)$ coordinate system using a Riemann solver for the MHD equations with enforced $\nabla \cdot \mathbf{B} = 0$ condition, and Alternating Direction Implicit scheme coupled with second-order upwind wave-propagation algorithm for the transport equation.

Accurate solution of the particle transport equation requires resolution of the small diffusion scales associated with the lowest energy particles. The advantage of having a locally refined grid near the shock was recognized by Dorfi and Drury (1987) in a work that used a 1-D two-fluid, cosmic-ray hydrodynamical model to compute the evolution of a spherical supernova remnant shock. Their approach used a partial differential equation to evolve the grid point distribution according to the gradients in the flow. Duffy (1994) used a local grid refinement to compute evolution of the cosmic-ray distribution function for 1-D planar shocks, and for a similar model Kang et al. (2001) used block adaptive mesh refinement (AMR) and a shock tracking method to capture the shock wave without intermediate transition points.

The discretized equations are evolved in time using a solution adaptive AMR grid hierarchy (Berger and LeVeque, 1998) that provides high spatial resolution near the shock. Figure 1 illustrates the evolution of the AMR grid structure in the vicinity of the shock. Flux functions are used to coordinate solutions at neighboring grid levels to ensure numerical conservation of physically conserved quantities. The code is parallelized using Message Passing Interface, suitable for distributed memory systems.

The MHD part of the code was tested on a number of problems, including MHD blast wave, Orzag-Tang MHD vortex problem and exact self-similar solutions. The transport equation solver was validated against exact solutions in the test-particle limit, and against numerical solutions of the cosmic ray acceleration problem in spherically symmetric shocks with zero magnetic field reported by Kang and Jones (1991).

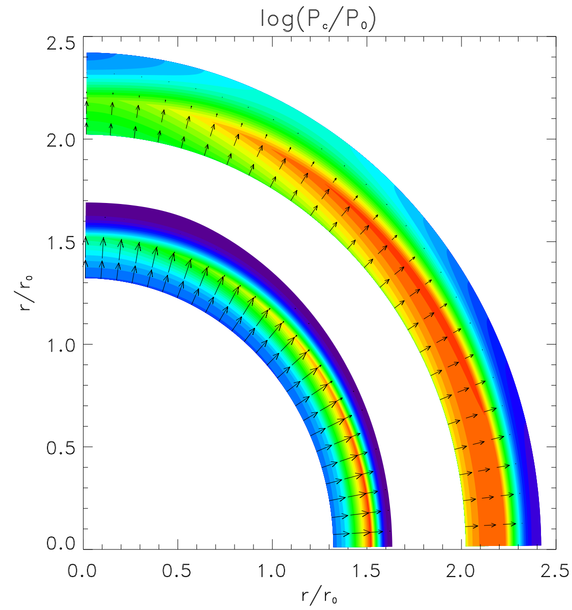


**Fig. 2.** Cosmic ray pressure (contour lines) and velocity field (vectors) in SNR shock at $t/t_0$ = 2.0 and 5.0. $\eta = 0.5$.

## 4 Computational Results

The initial condition for the plasma state is specified as a self-similar spherical Sedov blast wave. We use $\gamma_g = 5/3$, the energy of explosion is taken to be $E = 10^{51}\ erg$, and the interstellar density and pressure are set to $\rho_0 = 7 \times 10^{-27}$ $g\ cm^{-3}$ and $p_{g0} = 10^{-12}\ dyne\ cm^{-2}$ respectively. The solution is initialized at the time corresponding to the onset of the Sedov-Taylor phase, $t_0 = 6.1 \times 10^3\ yrs$, when the shock wave has expanded to the distance of $r_0 = 28.5\ pc$. The magnetic field strength upstream of the shock is chosen to be $B_0 = 5\ \mu G$. The shock is a parallel shock over the poles ($\theta = 0$), and a perpendicular shock at the equator ($\theta = \pi/2$). The initial condition for the distribution function is $f(\mathbf{r}, p, 0) = 0$.

In the calculations, the diffusion coefficients $\kappa_\parallel$ and $\kappa_\perp$, parallel and perpendicular to the magnetic field are taken as independent of momentum, in order to reduce computational time. In particular we take $\kappa_\parallel = \kappa_{\parallel 0} B_0/|\mathbf{B}|$ and $\kappa_\perp = \eta\kappa_\parallel$ where $\eta$ is a constant ($\eta < 1$). We take $\kappa_{\parallel 0} = 1.6 \times 10^{25}$ $cm^2 s^{-1}$. Since the magnetic field has no azimuthal component, there are no drift effects in the 2D model. Drift effects can play a role if $B_\phi \neq 0$.

In the test particle limit, the evolution of the SNR shock wave is dominated by the flow kinetic energy. The angle between the shock normal and the upstream magnetic field $\mathbf{B}$, increases continuously from pole ($\theta = 0$) to equator ($\theta = \pi/2$), and therefore the magnetic field pressure downstream is largest at the equator, for the perpendicular shock configuration. When the shock expands to $\sim 75\ pc$, magnetic stresses become strong enough to influence flow dynamics. This leads to a non-spherical shock, in which the compression ratio $r_c$ is larger at the pole than at the equator ($r_{cp} = 3.4$ and $r_{ce} = 2.9$).

When the cosmic ray back-reaction on the thermal component of the plasma is taken into account, the shock wave structure is modified. The effect is strongest at the equator, where the shock normal is perpendicular to the magnetic field lines and diffusion in the radial direction is governed by $\kappa_\perp$. Figure 2 shows the evolution of the cosmic ray pressure at the shock for the ratio $\eta = \kappa_\perp/\kappa_\parallel = 0.5$ and $v_{inj}$ dependent only on the shock speed. Figure 3 shows the radial variation of $p_c$ and $p_g$ in the vicinity of the shock at time $t/t_0 = 4$, both at the equator ($\theta = \pi/2$) and at the pole ($\theta = 0$), for models with different $\eta$. The cosmic ray pressure is the dominant pressure at the equator ($p_c/p_g \sim 3$), whereas the gas pressure dominates at the pole ($p_c/p_g \sim \frac{1}{3}$).

Figure 4 illustrates the evolution of the energetic particle distribution function at the shock both at the pole and at the equator at times $t/t_0$ = 1.75, 2.5 and 4.0, for the case where injection speed is given by $v_{inj} = \xi v_{sh}(\kappa_\parallel/\kappa_{nn})^{1/2}$. The injection is parametrised in terms of the parameter

$$\epsilon = \frac{4\pi p_{inj}^3 f(\mathbf{r}, p_{inj}, t)}{\rho_0/m_p} \frac{r_c - 1}{3r_c}. \quad (10)$$

The diffusion coefficient was taken as independent of $p$ and the ratio $\kappa_\perp/\kappa_\parallel = 0.2$. As shown in Figure 4, the acceleration rate is faster at the equator where $\kappa_{nn} = \kappa_\perp$, than at the pole, where $\kappa_{nn} = \kappa_\parallel$. A similar result was obtained in the test particle simulations of Jokipii and Ko (1987), (see also Jokipii (1987)) who pointed out that the particle acceleration rate is significantly faster in quasi-perpendicular shocks than in quasi-parallel shocks, if $\eta << 1$.

Note that the distribution function is an order of magnitude smaller at the equator than at the poles. This is a consequence of the fact that the injection speed is substantially larger at the equator than at the poles, and the assumed Maxwellian form of the distribution function at the injection energy.

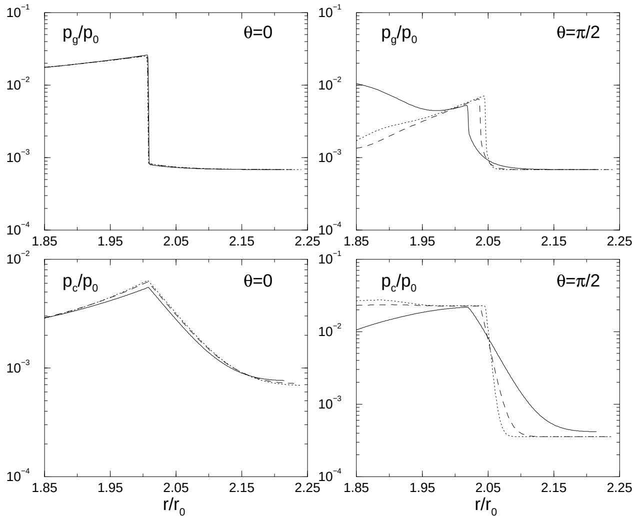


**Fig. 3.** Cosmic-ray and thermal pressure at $t/t_0$ = 4.0 for models with $\eta = 0.5$ (solid line), $\eta = 0.2$ (dashed line), $\eta = 0.1$ (dotted line).

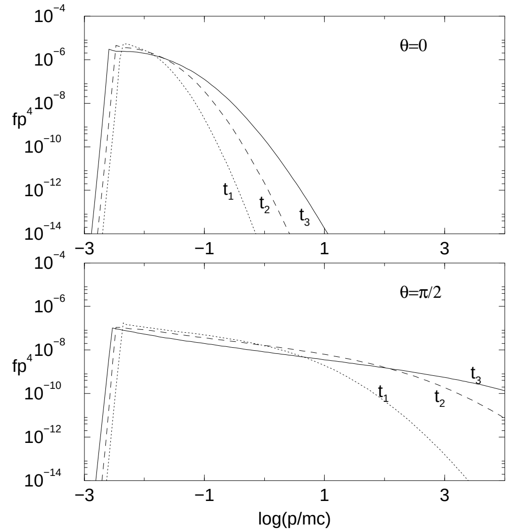


**Fig. 4.** Distribution function downstream of the shock for angles $\theta = 0$ and $\theta = \pi/2$ at times $t_1/t_0$ = 1.75, $t_2/t_0$ = 2.5 and $t_3/t_0$ = 4.0. $\eta = 0.2$.

## 5 Concluding Remarks

It is clear from Figure 4 that the magnetic field geometry and $\eta = \kappa_\perp/\kappa_\parallel$ will play an important role in determining the maximum energy obtained by the accelerated particles near the shock, depending on the phase of evolution of the remnant. For example, in the lower panel in Figure 4, the break in the spectrum at $t = t_2 = 1.525 \times 10^4$ years at the shock in the equatorial region ($\theta = \pi/2$, $r_{sh} \sim 45$ pc), occurs at $p = p_b \approx 10^2$mc $= 93.8$ GeV/c, whereas at the pole ($\theta = 0$), the corresponding break occurs at $p_b \approx 10^{-1.5}$ mc $= 29.6$ MeV. Thus, the particles are accelerated to $\sim 10^{3.5}$ greater energies at the equator than at the poles. This difference in the increased acceleration rate at quasi-perpendicular shocks is well known in test particle acceleration theory (e.g. Jokipii (1987), Jokipii and Ko (1987)), but current, spherically symmetric models of cosmic ray modified SNR shocks cannot accomodate these effects. Our model shows that anisotropic diffusion is important in the fully nonlinear theory. The difference in the acceleration rates at the pole and equator has important implications for synchrotron and radio emission from SNR remnant shocks (e.g. Reynolds and Ellison (1991); Ratkiewicz et al (1994)), and also for gamma ray emission from SNR remnants (e.g. Baring et al., (1999)).

It is of interest to extend the present calculations to include more realistic diffusion coefficients that increase with the particle energy (e.g. $\kappa_\parallel \propto p^{\frac{1}{3}} v/c$ for Kolmogorov turbulence, or $\kappa \propto pv/c$ for Bohm diffusion).

*Acknowledgements.* Computations were performed on supercomputer facilities of the University of Arizona Center for Computation and Information Technology. The work of GMW was supported in part by NASA grant NAG5-5180. The work of JRJ was supported in part by NSF grant ATM-9616547.

## References


Baring, M.G., Ellison, D.C., Reynolds, S.P., Grenier, I.A. and Goret, P. 1999, *Ap. J.*, **513**, 311-338.

Berezhko, E.G., Elshin, V.K., Ksenofontov, L.T. 1996, *Astronomicheskii Zhurnal*, **73** no.2, 176–88.

Berger, M.J. and LeVeque, R.J. 1998, *SIAM J. Numer. Anal.* **35**.

Dorfi, E. A, and Drury, L. O'C. 1987, *J. Comput. Phys.*, **69**, 175.

Dorfi, E. A 1990, Astron. Astrophys., **234**, 419.

Duffy, P. 1994, *Ap. J. Suppl.*, **90**, 981.

Falle, S.A.E.G. and Giddings, J.R. 1987, *Mon. Not. R. Astr. Soc.* **225**, 399.

Gieseler, U.D.J., Jones, T.W. and Kang, H. 1999, *Proc. 26th. Int. Cosmic Rays Conf.*, **4**, 419-22.

Jokipii, J.R. 1987, *Ap. J.*, **313**, 842-846.

Jokipii, J.R. and Ko, C.M. 1987, *Proc. 20th Int. Cosmic Ray Conf.*, Moscow, OG 8.1-8.

Jones, T.W. and Kang, H. 1990, *Ap. J.*, **363**, 499-514.

Kang, H. and Jones, T. W. 1991, *Mon. Not. Roy. Astron. Soc.*, **249**, 439-51.

Kang, H., Jones, T. W., LeVeque R.J. and Shyue, K.M. 2001, *Ap. J.*, **550**, 737-751.

Krymskii, G.F. 1964, *Geomagn. and Aeron.*, **4**, 977.

Malkov, M. and Völk, H. 1995, *Astron. Astrophys.* **300**.

Parker, E.N. 1965, *Planet. Space Sci.*, **13**, 9.

Ratkiewicz, R., Axford, W.I. and McKenzie, J.F. 1994, *Astron. Astrophys.*, **291**, 935-42.

Reynolds, S.P. and Ellison, D.C. 1991, *Ap. J.*, **399**, L75-78.

Skilling, J. 1975, *Mon. Not. Roy. Astron. Soc.*, **172**, 557.

Zakharian, A.R. 2000, Ph.D. thesis, University of Arizona.